International Journal of Pharmaceutics 379 (2009) 59–66

Contents lists available at ScienceDirect

International Journal of Pharmaceutics

journal homepage: www.elsevier.com/locate/ijpharm

Following the surface response of caffeine cocrystals to controlled humidity storage by atomic force microscopy

A.M.C. Cassidy, C.E. Gardner, W. Jones*

University of Cambridge, Lensfield Road, Cambridge CB2 1EW, UK

ARTICLE INFO

Article history:
Received 17 November 2008
Received in revised form 29 May 2009
Accepted 9 June 2009
Available online 17 June 2009

Keywords:
Pharmaceutical material
Cocrystal
Atomic force microscopy (AFM)
Caffeine

ABSTRACT

Active pharmaceutical ingredient (API) stability in solid state tablet formulation is frequently a function of the relative humidity (RH) environment in which the drug is stored. Caffeine is one such problematic API. Previously reported caffeine cocrystals, however, were found to offer increased resistance to caffeine hydrate formation. Here we report on the use of atomic force microscopy (AFM) to image the surface of two caffeine cocrystal systems to look for differences between the surface and bulk response of the cocrystal to storage in controlled humidity environments. Bulk responses have previously been assessed by powder X-ray diffraction. With AFM, pinning sites were identified at step edges on caffeine/oxalic acid, with these sites leading to non-uniform step movement on going from ambient to 0% RH. At RH > 75%, areas of fresh crystal growth were seen on the cocrystal surface. In the case of caffeine/malonic acid the cocrystals were observed to absorb water anisotropically after storage at 75% RH for 2 days, affecting the surface topography of the cocrystal. These results show that AFM expands on the data gathered by bulk analytical techniques, such as powder X-ray diffraction, by providing localised surface information. This surface information may be important for better predicting API stability in isolation and at a solid state API–excipient interface.

1. Introduction

Understanding the surface structure and morphology of pharmaceutical materials contributes to an understanding of surface reactivity and so is of critical importance to the pharmaceutical industry (Buckton, 1997; Cui, 2007). Surface reactivity will affect drug stability during the process of tablet formulation, where grinding and compaction give rise to many surface–surface interfaces where reactions can occur. Recent efforts have been made to develop techniques and protocols for analysing the surfaces of soft organic materials, as understanding these surfaces may help to shed light on the interactions which occur between crystals and their surrounding environments (Roberts, 2005; Tian et al., 2006). The relative humidity (RH) surrounding a crystal is of particular significance since increasing RH allows for greater molecular mobility, thereby influencing the stability of pharmaceutical materials (Ahlneck and Zografi, 1990; Dalton and Hancock, 1997; Airaksinen et al., 2005).

One way of improving the inherent stability of a pharmaceutical material is by exploiting the benefits offered by cocrystal engineering (Almarsson and Zaworotko, 2004; Trask, 2007). Cocrystals are multicomponent crystals and cocrystal engineering allows for the design of an appropriate multicomponent crystalline material which can introduce new or improved physical properties to a pharmaceutical drug. Previous work (Trask et al., 2005) showed it was possible to engineer a caffeine cocrystal which would circumvent the tendency of caffeine to form caffeine hydrate (Pirttimaki and Laine, 1994; Edwards et al., 1997). Despite the significant activity in the field of cocrystal discovery (Almarsson and Zaworotko, 2004; Vishweshwar et al., 2006), however, little attention has focused on the surface morphology of these complex materials.

Atomic force microscopy (AFM) (Binnig et al., 1986) has proved to be a valuable tool in understanding the surface properties of pharmaceutical materials (Li et al., 2000; Berard et al., 2002; Price and Young, 2004; Liu et al., 2007; Turner et al., 2007; Jones et al., 2008). As AFM analysis, used under the appropriate conditions, is non-destructive it allows for the collection of topographic data regarding the state of a surface over extended time periods.

In the work presented here, AFM has been used in conjunction with scanning electron microscopy (SEM) and optical microscopy. This range of imaging scale has allowed quantitative topographical observations to be made over the same scan area on a surface for periods up to 7 days. The cocrystals chosen for surface analysis were the caffeine/oxalic acid and caffeine/malonic acid cocrystals which had been previously reported by Trask et al. (2005), see Table 1. Caffeine/oxalic acid was shown by powder X-ray diffraction (PXRD) to offer increased resistance to caffeine hydrate formation when compared to anhydrous caffeine. Anhydrous β-caffeine was shown

* Corresponding author. Tel.: +44 1223 336468; fax: +44 1223 762829.
E-mail address: wj10@cam.ac.uk (W. Jones).

0378-5173/$ – see front matter © 2009 Elsevier B.V. All rights reserved.
doi:10.1016/j.ijpharm.2009.06.009

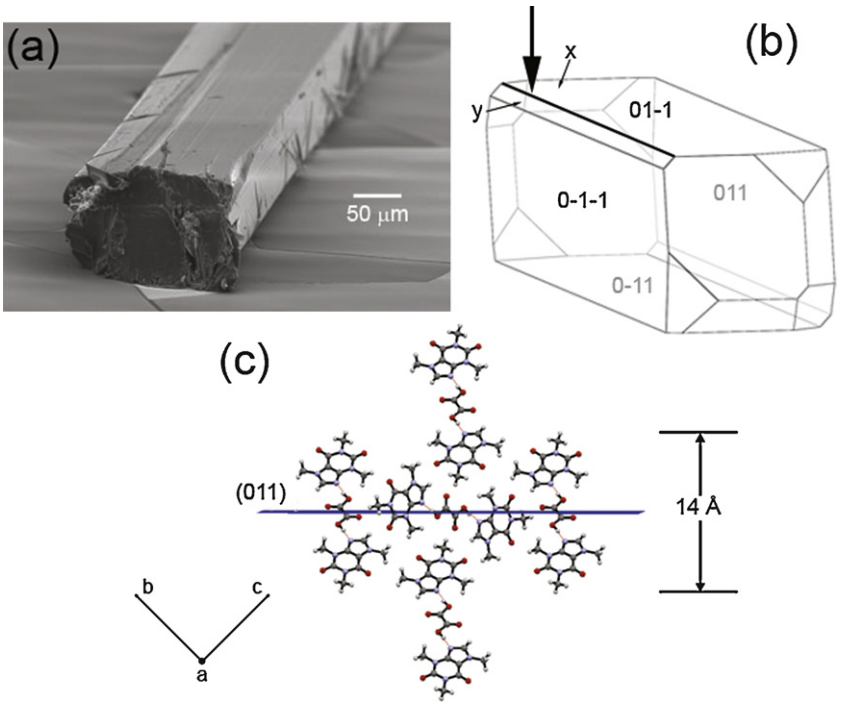

Fig. 1. (a) SEM showing the needle morphology of a freshly prepared caffeine/oxalic acid cocrystal. (b) Morphology of caffeine/oxalic acid cocrystal simulated using a BFDH prediction. The dominant faces are labeled, all of these faces express the same functionality at their surface. The alignment of faces *x* and *y* is also indicated, with the intense line marking the interface between the two faces. (c) An example of the chemical functionality expressed at the (0 1 1) face.

to convert to caffeine hydrate partially after 1 day and completely after 3 days at 98% RH. Caffeine/oxalic acid was shown to remain stable after 7 weeks storage at 98% RH, whereas caffeine/malonic acid showed more limited stability only to 75% RH for a similar period of time and indeed partially converted to caffeine hydrate after only 1 week at 98% RH. The aim of this work was therefore two-fold: firstly, to use AFM to characterise the surface of a cocrystal material; and secondly, to exploit the potential of AFM to highlight any differences between bulk and surface stability.

2. Materials and methods

2.1. Materials

Cocrystals were grown using methods described in detail elsewhere (Trask et al., 2005). Caffeine and either oxalic acid or malonic acid (research grade, Sigma–Aldrich) were manually ground in a 2:1 (by molarity) homogeneous mixture. 100 mg divisions were dissolved, with heating, in the minimum volume of the following solvent mixtures: 1:1 chloroform:methanol for caffeine/oxalic acid cocrystals and 15:1 nitromethane:methanol for caffeine/malonic acid cocrystals. Cocrystal precipitation was left to occur under ambient conditions (22 °C). Experimental PXRD patterns were compared with simulated patterns to confirm the composition of these materials.

Table 1
Crystallographic data for caffeine cocrystals (Trask et al., 2005).

	Caffeine/oxalic acid (2:1)	Caffeine/malonic acid (2:1)
Experimental formula	$2(C_8H_{10}N_4O_2)\cdot C_2H_2O_4$	$2(C_8H_{10}N_4O_2)\cdot C_3H_4O_4$
Formula weight	478.44	492.46
Crystal system	Monoclinic	Orthorhombic
Space group	$P2_1/c$	$Fdd2$
a (Å)	4.41430(10)	30.3992(12)
b (Å)	14.7701(5)	31.2845(16)
c (Å)	15.9119(6)	4.6739(2)
α (degree)	90	90
β (degree)	96.4850(10)	90
γ (degree)	90	90

2.2. Humidity control

Desiccators containing P_2O_5 and saturated NaCl and K_2SO_4 salt solutions were used to maintain 0%, 75% and 98% relative humidity environments, respectively. The RH was monitored using humidity indicator cards (Sigma–Aldrich). To measure the surface response of individual samples, single, needle-shaped crystals (*ca.* 3–4 mm in length) were prepared for AFM imaging, as described below, and stored.

2.3. AFM

AFM images were recorded using a Multimode AFM (operated by a Nanoscope IIIa controller, interfaced with a Quadrex extender module, Veeco Instruments, Santa Barbara). The stage was equipped with a video microscope to facilitate exact sample positioning, allowing the cantilever to be returned to the same area on a surface. Crystals were only removed from contact with the mother liquor just prior to examination. Individual cocrystals were dried on filter paper before being fixed to glass coverslips using superglue. The coverslips were then attached to stainless steel AFM sample discs using sticky tabs. Samples were imaged in air with either a J (180 μm × 180 μm maximum scan size) or E (13 μm × 13 μm maximum scan size) scanner under normal conditions of room temperature (22 °C), atmospheric pressure and approximately 40% relative humidity. All imaging occurred within 2 h of removing the sample from the desiccator. There was no evidence that this time away from the target RH resulted in changes to surface structure. All images were recorded in contact mode using commercially available sharpened Si_3N_4 probes with a nominal spring constant of 0.06 N/m and an average radius of curvature of 10 nm (Veeco). The tip–sample contact force was minimised by optimising the deflection setpoint. Topographical images were collected at a scan rate of 1 Hz. Height,

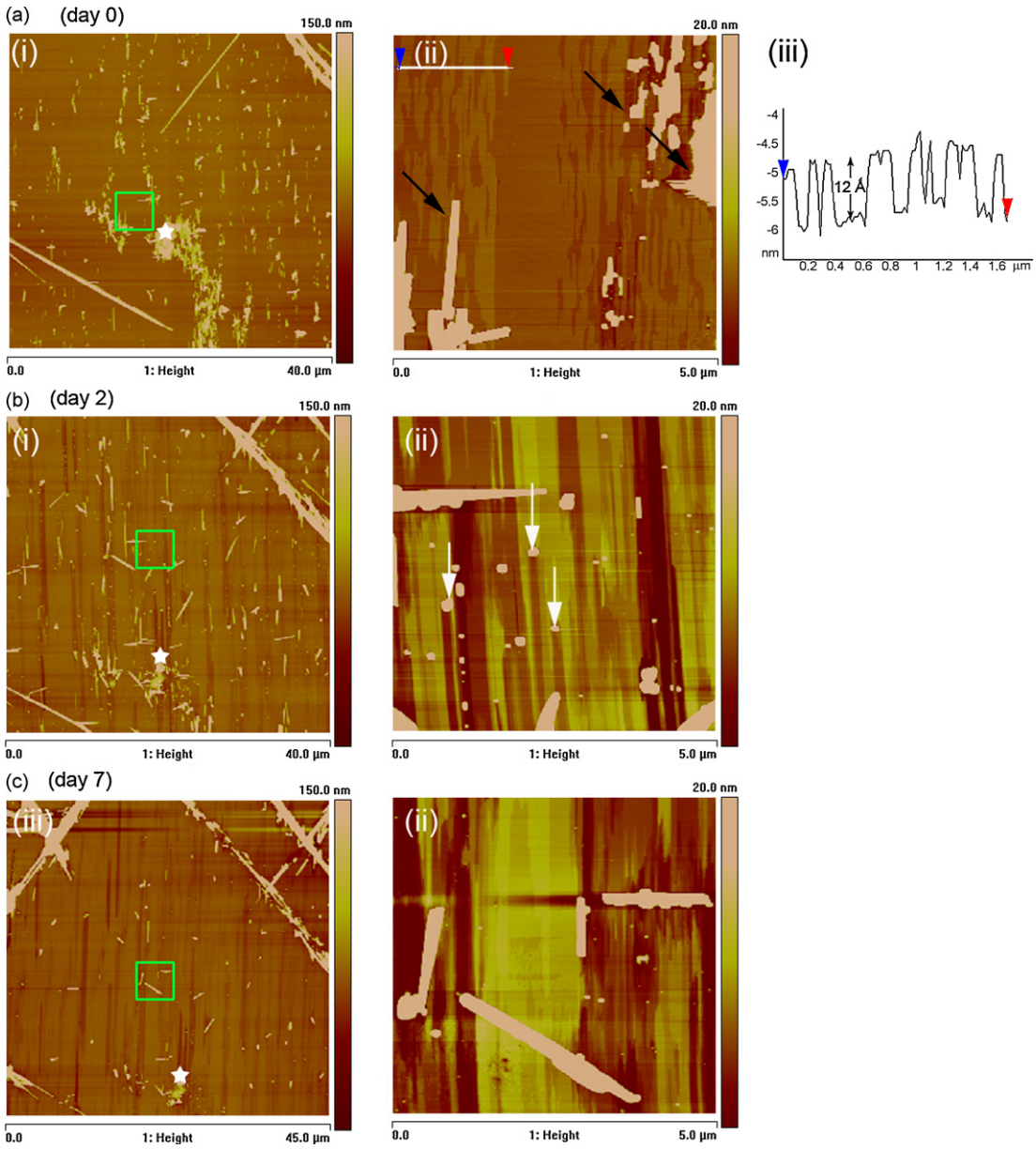

Fig. 2. Representative AFM height images of a caffeine/oxalic acid cocrystal stored in a desiccator at 0% RH. The green square drawn on each of the larger scans indicates the area shown in the adjacent 5 μm × 5 μm image. The white stars on the larger images indicate the same location on each surface. (a) Day 0, immediately after the crystal was prepared for analysis, (ii) the black arrows indicate unidentified surface material (iii) line section corresponding to the white line shown in (ii). (b) Day 2 (ii) the white arrows indicate pinning sites where surface features (*ca.* 20–60 nm in height) have grown normal to the crystal face. (c) Day 7 (ii) surface features are reduced in height and frequency.

deflection and friction data were collected simultaneously. The scans were analysed using Nanoscope ™ software version 6.13. Each image was processed using the first order flatten command within the software to remove the effect of tilt on the sample.

2.4. SEM

Scanning electron microscopy was performed using a JEOL JSM5510LV. Samples were mounted on brass SEM stubs with carbon tape and coated with a thin layer of gold (approximately 15 nm) using an Emitech K550 Sputter coater.

2.5. PXRD

PXRD patterns were collected on a Phillips PW3710 diffractometer with nickel-filtered Cu Kα radiation. Fixed width divergence and anti-scatter slits of sizes 0.5 and 1 in., respectively, were used. X-ray intensities were measured with a scanning real time multiple strip (RTMS) X'Celerator detector with an active length of 9 mm, covering *ca.*2.127° 2θ. Samples were typically analysed between 5 and 60° 2θ with a step size of 0.008° 2θ and a total scan time of *ca.*5 min. Samples were prepared by grinding when necessary and supporting on glass slides. BFDH simulations were performed using Mercury (ver. 2.2, CCDC, Cambridge, UK) and single crystal diffraction data gathered by Trask et al. (2005).

3. Results and discussion

3.1. Caffeine/oxalic acid

The needle morphology of a caffeine/oxalic acid cocrystal is illustrated by the SEM image in Fig. 1(a). This habit and the alignment of the unit cell axes were found to be in good agreement with the habit

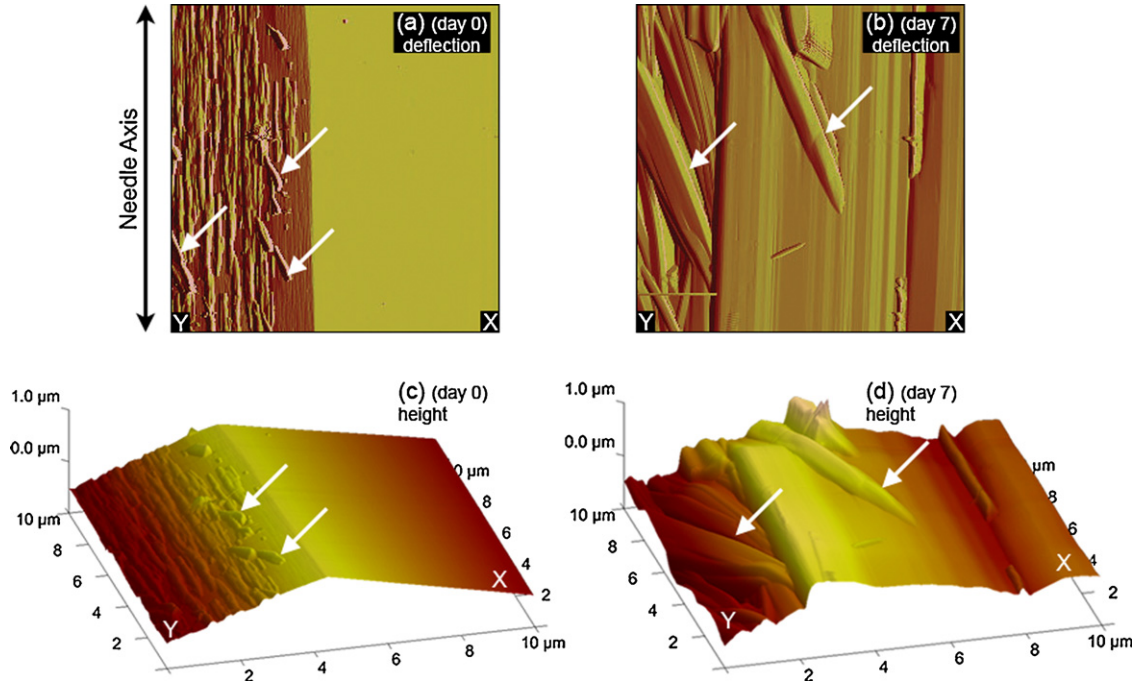

Fig. 3. Representative AFM images of a caffeine/oxalic acid cocrystal stored in a desiccator at 75% RH. All images were recorded at the interface between faces *x* and *y* as indicated by the arrow in Fig. 1(b). (a) Deflection image recorded at day 0, immediately after the sample was prepared for analysis. (b) Deflection image recorded at day 7. (c) Corresponding 3D topography representation of (a). (d) Corresponding 3D topography representation of (b).

predicted by a BFDH simulation (Fig. 1(b)). The simulation showed the (0 1 − 1), (0 1 1), (0 − 1 1) and (0 − 1 − 1) faces to be the dominant crystal faces. We assume these were the faces most likely to be accessible to the AFM tip. The computer simulation indicated these faces to have similar exposed chemical functionality, an example of which is given in Fig. 1(c). Samples were studied in triplicate and while conclusions are based on these three separate studies, for clarity images shown in a particular figure relate to the same sample.

Fig. 2 shows typical AFM images of the surface of a caffeine/oxalic acid cocrystal at different stages of exposure to 0% RH. Large area scans are included to show that the same area of the surface was imaged each day, while smaller 5 μm × 5 μm images are included to better illustrate the observed nanoscale changes to surface topography. The surface is shown at day 0, immediately after removal from contact with the mother liquor (a) and after 2 days (b) and 7 days (c) storage, in a desiccator, at 0% RH. Trenches aligned along the needle axis, were observed on the freshly prepared surface at day 0. The trench walls were measured to be between 10 and 12 Å in height (Fig. 2(a)iii), and as such were presumed likely to result from the presence of single molecular layers. The surface material indicated by black arrows in Fig. 2(a)ii, ranged in height from 30 to 180 nm. Such surface material was found to be a common feature on all caffeine/oxalic acid cocrystal surfaces studied and was considered to be fixed to the surface since it was not removed by drying the samples with filter paper during sample preparation nor was it displaced by repeated movement of the AFM tip during scanning. It is believed to result from the rapid evaporation of trace solvents when the cocrystal is first removed from contact with the mother liqour.

After 2 days storage at 0% RH pinning sites were observed on the cocrystal surface. The pinning sites were identified by the growth of material normal to the crystal surface, localised to the ends of trenches. Examples of such peaks, ranging in height from 20 to 60 nm, are marked with white arrows in Fig. 2(b)ii.

The surface trenches, shown in Fig. 2(a)ii, increased in depth from an average of 10 Å at day 0 to between 30 and 100 Å by day 2. This was accompanied by an increase in the width of the trenches from an average of 140 nm on day 0 to an average of 760 nm by day 2. The localised growth of peaks accompanied by the increase in trench size resulted in an increase in surface roughness from 2 nm at day 0 to 5 nm by day 2. These surface roughness values were recorded on the same 10 μm × 10 μm square, within the original larger scale scan area. Surface roughness is defined as:

$$R_{\mathrm{RMS}} = \left[\frac{1}{N}\sum_{n=1}^{N}(y_n)^2\right]^{1/2} \quad (1)$$

where N is the number of data points and y_n is the deviation in relative vertical height from the average height. Although exposure at 0% RH for 7 days led to a continued increase in trench length and width (average trench width of 910 nm by day 7, Fig. 2(c)i), the surface roughness value fell to *ca.* 2 nm after prolonged storage. This reduction is attributed to a decrease in the number of features growing normal to the crystal surface, evidenced by the day 7 image in Fig. 2(c)ii.

The AFM images indicate that the surface of a caffeine/oxalic acid cocrystal changes noticeably in response to storage at 0% RH. The surface "reconstructions" are, we believe, attributable to the removal of surface water layers and any residual solvents and the subsequent incorporation of previously dissolved material into the crystal surface. It is possible that on the surface of a cocrystal (where, by definition, at least two molecular species are present) the adsorption of an incorrect species may produce a pinning point. An incorrect species could be an impurity or one of the cocrystal components aligned out of sequence. Pinning sites are regularly observed when impurities are added as growth modifiers to organic crystals (Keel et al., 2004; Thompson et al., 2004). If steps were prevented from propagating parallel to the crystal face then instead movement could be directed normal to the face, resulting in the observed growth. This effect is likely to be pronounced by storage at 0% RH where the removal of previously adsorbed water and residual solvent causes surface reconstruction in an environment where

there is reduced molecular mobility, making it more difficult for a dynamic step to overcome a pinning point. It was demonstrated that there is a variation with time in both surface roughness (and consequently surface area) and in exposed crystallographic faces (by the growth of peaks and deepening of trenches) in response to storage at 0% RH. These changes could prove significant in terms of the energy landscape which the surface presents at a pharmaceutically relevant solid state interface.

Fig. 3 shows typical AFM topography and deflection images which illustrate the response of a caffeine/oxalic acid cocrystal to storage at 75% RH. It was fortunate that this particular sample allowed for images to be recorded at the interface of two distinct crystal faces, identified as *x* and *y* in Fig. 1(b). As expected, face *x*, to the right hand side of Fig. 3(a) and (c) is similar to that shown in Fig. 2, having a surface roughness of approximately 4 nm and trenches on the scale of a molecular layer. These trenches are not visible in Fig. 3 due to a change in the height scale used. Face *y*, however, is uneven with a much larger surface roughness of 107 nm. After 7 days storage at 75% RH face *x* showed clear signs of step rearrangement. Molecular layer steps were replaced by multimolecular layer steps, measuring up to 19 nm in height. Surface material (similar to that identified in Fig. 2(a), but not shown here) was observed to rearrange and gave regular, triangular- and rectangular-shaped features indicative of surface recrystallization. This effect, however, was much more pronounced at 98% RH as shown later in Fig. 4.

The features which contributed to the high surface roughness values for face *y*, in Fig. 3(a) and (c) were predominantly aligned parallel to the needle axis of the crystal. Also present were features which appeared at *ca.* 25° to the needle axis, marked with arrows in Fig. 3(a) and (c). It was these features which were most affected by storage at 75% RH as evidenced by Fig. 3(b) and (d), where they have again been marked with arrows. These features appear to traverse the entire crystal face and encroach onto the adjacent face. The orientation of this molecular rearrangement in one specific direction is notable. Moreover, the contrast in magnitude between the degrees of molecular movement obtained on two adjacent faces is marked.

The 75% RH environment evidently facilitated a large degree of molecular mobility. Unlike at 0% RH where the evolution of pinning sites highlighted the restrictions on molecular mobility, the 75% RH environment promoted significant surface reconstruction.

Fig. 4 shows representative AFM topographic images of a dominant caffeine/oxalic acid cocrystal face and its response to storage at 98% RH. Further evidence of the surface material mentioned previously can be seen. The background entrenched surface is masked by the overall height scale of the images, but the trench height measured *ca.* 10 Å. There was a reduction in surface material over time which was accompanied by a corresponding linear decrease in the surface roughness of the sample, with surface roughness, measured over a 10 μm × 10 μm square, dropping from 61 nm at day 0 to 12 nm by day 7. This loss of surface material is attributed to an annealing-like process facilitated by the high RH. Although this level of reconstruction was not detected by PXRD analysis, subsequent dynamic vapour sorption (DVS) measurements (using a DVS-1 from Surface Measurement Systems with a 0.05 μg resolution mass balance, sample mass 18 mg) indicated a 0.1% hysteresis in sample mass between the sorption and desorption isotherms. This small mass loss concurred with the conclusion that surface recrystallization had occurred. Although this does suggest that surface material was of a less stable phase than the bulk crystalline material, it does not allow for unambiguous characterisation of this material.

3.2. Caffeine/malonic acid

Fig. 5(a) shows the needle morphology of a caffeine/malonic acid cocrystal. This habit was found to be in agreement with a BFDH computer simulated morphology (Fig. 5(b)). The labeled faces present similar exposed chemical functionality, an example of which is shown in Fig. 5(c), and were assumed to be the faces accessible to the AFM tip.

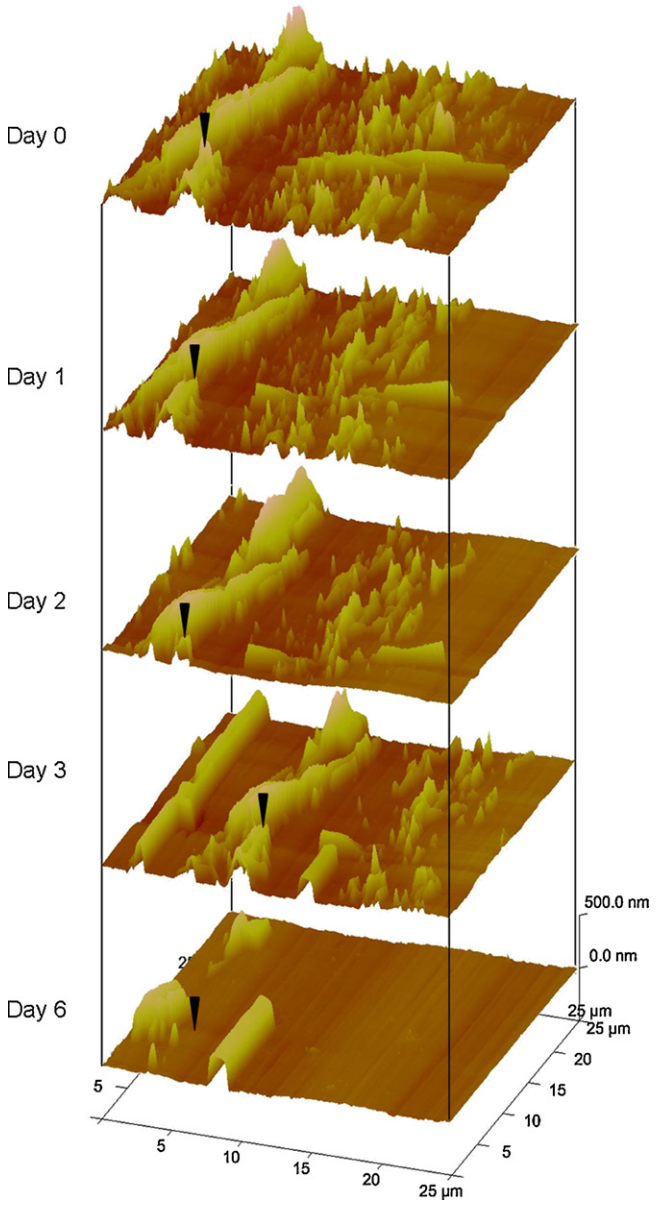

Fig. 4. Representative AFM images of a caffeine/oxalic acid cocrystal stored in a desiccator at 98% RH. All images were recorded as near to the same scan site as possible. The black arrow marks the same point of reference on each image. The surface material present in the day 0 image is seen to anneal into the surface by day 6.

Fig. 6(a) shows a representative AFM topographic image of a caffeine/malonic acid cocrystal surface. The white box highlights an area which was damaged by the AFM tip while scanning the surface, despite minimisation of the applied force. This was taken as preliminary evidence that caffeine/malonic acid presented a softer surface for imaging than caffeine/oxalic acid, as such tip induced surface damage was not observed in the case of the latter. Like caffeine/oxalic acid, the caffeine/malonic acid surface showed evidence of pinning sites. However, here the pinning sites occurred at the front of molecular height steps (measured at *ca.* 5–7 Å in height) as they propagated along the needle axis, indicated by black arrows in Fig. 6 (a). This gave these steps a serrated edge in con-

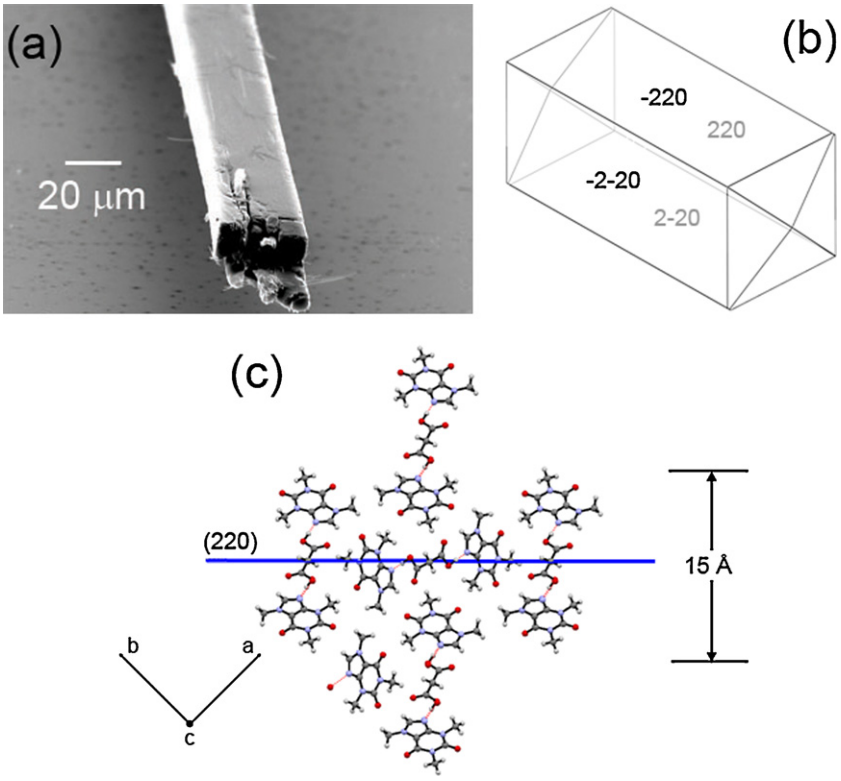

Fig. 5. (a) SEM showing the needle morphology of a caffeine/malonic acid cocrystal. (b) Morphology of caffeine/malonic acid cocrystal simulated using a BFDH prediction. (c) An example of the chemical functionality expressed at the (2 2 0) face.

trast to the entrenched surface observed on caffeine/oxalic acid. Fig. 6(b) shows the same crystallographic face after 2 days storage at 75% RH. The 'fibres' observed were aligned along the *c*-axis of the unit cell (also the crystal needle axis). These fibres ranged in width from 0.3 to 0.6 μm. Multimolecular layer steps (*ca.* 2–4 nm in height) were observed along the length of these fibres suggesting that crystallinity was preserved. Little change was observed in the morphology of these fibres with increased storage time. The SEM image in Fig. 7(a) recorded after 7 days storage at 75% RH shows that the evolution of these fibres was not confined to the surface of the caffeine/malonic acid cocrystals. A comparison of the SEM images in Figs. 5(a) and 7(a) indicates that although the cocrystal has retained its overall needle habit, the fibres which evolved at 75% RH dominate the complete crystal morphology.

The changes reported to the morphology of the caffeine/malonic acid cocrystals are in contrast with the PXRD measurements. PXRD analysis undertaken by Trask et al. (2005), indicated that these cocrystals were unchanged after 7 weeks storage at 75% RH. Here, although the chemical stability of the cocrystal structure was not compromised, the physical stability of the cocrystal structure was

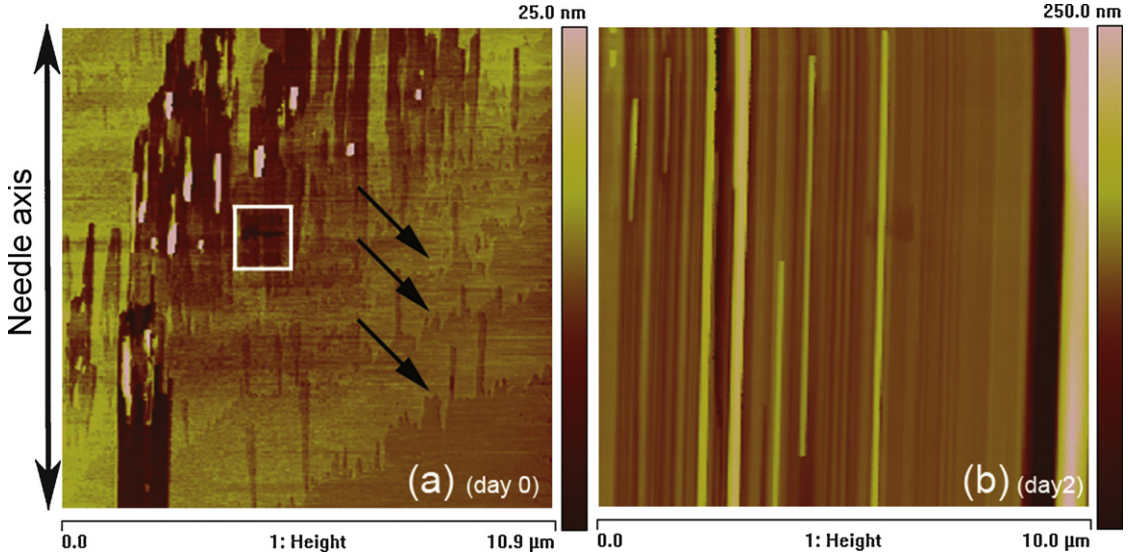

Fig. 6. Representative AFM images of a caffeine/malonic acid cocrystal stored in a desiccator at 75% RH. (a) Height image recorded at day 0, immediately after the sample was prepared for analysis. The white square marks out tip damage. The black arrows indicate serrated step edges, indicative of pinning sites. (b) Height image recorded at day 2 demonstrating the fibrous nature of the cocrystal, exposed after storage at high humidities.

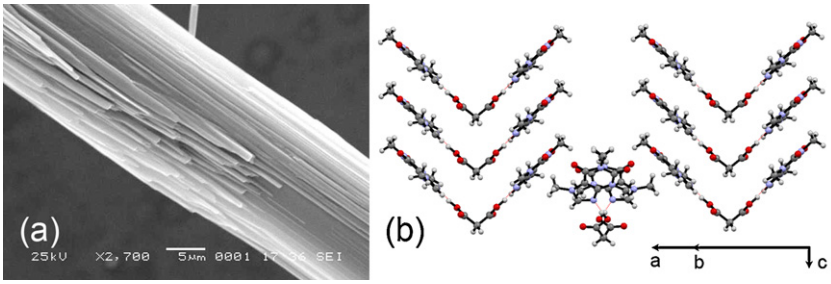

Fig. 7. (a) An SEM image of a caffeine/malonic cocrystal stored in a desiccator at 75% RH for 7 days. (b) The crystal packing diagram for caffeine/malonic acid showing stacks of trimeric units stacked along the *c*-axis.

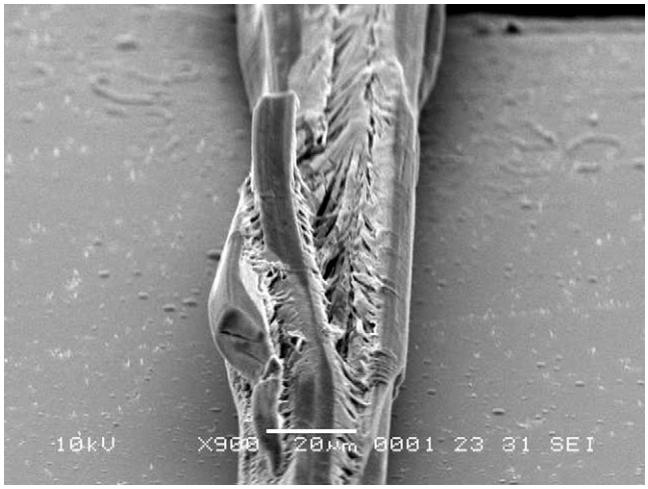

Fig. 8. SEM image of a caffeine/malonic cocrystal stored for 7 days at 98% RH. The proposed evolution of caffeine hydrate made AFM imaging impossible.

clearly affected by the 75% RH environment. The crystal packing diagram, Fig. 7(b), shows that molecules are arranged in stacks of trimeric units along the needle axis of the cocrystal. It is possible that the high RH environment allowed for an uptake of water between these stacks via a capillary absorption mechanism. DVS measurements showed a 0.2% mass increase at 75% RH (25 mg sample mass). AFM and SEM results showed that this water uptake led to the development of anisotropic fibres, correlating with the anisotropic way in which trimeric units stack in the packing diagram. The resulting exposure of the underlying fibrillar nature of the caffeine/malonic acid cocrystal could act as a precursor to the formation of caffeine hydrate at higher RH environments. Water has previously been reported to be most mobile along the needle axis in caffeine hydrate (Byrn and Lin, 1976; Griesser and Burger, 1995).

The SEM in Fig. 8 shows a caffeine/malonic acid cocrystal stored at 98% RH for 7 days. DVS measurements showed a 0.5% mass increase at 90% RH after 20 h. The complete rearrangement of the caffeine/malonic acid morphology, presumably caused by the formation of caffeine hydrate previously reported (Trask et al., 2005), combined with the formation of a water layer on the surface of the cocrystals at 98% RH inhibited AFM imaging which might have allowed us to follow this process.

4. Conclusions

The study reported here has shown that AFM, combined with other microscopy techniques, can add potentially useful data concerning the stability of caffeine/carboxylic acid cocrystal materials to that gained by bulk analysis techniques such as PXRD. The results give an initial impression of the behaviour of organic cocrystal material in response to controlled RH storage. The prevalence of pinning sites on both materials, particularly after the removal of surface water layers upon storage at 0% RH, may potentially be characteristic of cocrystals in general. Due to their multicomponent construction, the presence of more than one molecular species available to be adsorbed at growth sites is, by definition, possible. As such, cocrystals may exhibit an extended number of active sites (or a reduced tendency to form flat extended terraces).

A high degree of molecular mobility was observed on the surface of caffeine/oxalic acid cocrystals when samples were stored in high ($\geq$ 75%) RH environments. DVS and AFM data suggested that this mobility may have led to recrystallization phenomena on the crystal surfaces.

A link between the anisotropic packing of caffeine/malonic acid and its tendency to anisotropically absorb water prior to caffeine hydrate formation was demonstrated. The use of microscopic techniques allowed for observation of this tendency before it could be detected by PXRD. Present work aimed at assessing the chemical nature of surface changes, exploiting both spectroscopic and microscopic techniques, is underway.

Acknowledgments

The authors wish to thank Barry Aldous (Pfizer Global R&D) for running DVS experiments, Dr. Evgenyi Shalaev, Dr. Ken Waterman, Dr. Sheri Shamblin and Dr. Tony Affret for helpful discussions. Thanks also to Pfizer Institute for Pharmaceutical Material Science for providing funding for this study.

References

Ahlneck, C., Zografi, G., 1990. The molecular basis of moisture effects on the physical and chemical stability of drugs in the solid state. Int. J. Pharm. 62 (2–3), 87–95.
Airaksinen, S., Karjalainen, M., Shevchenko, A., Westermarck, S., Leppnen, E., Rantanen, J., Yliruusi, J., 2005. Role of water in the physical stability of solid dosage formulations. J. Pharm. Sci. 94 (10), 2147–2165.
Almarsson, O., Zaworotko, M.J., 2004. Crystal engineering of the composition of pharmaceutical phases. Do pharmaceutical co-crystals represent a new path to improved medicines? Chem. Commun. 17, 1889–1896.
Berard, V., Lesniewska, E., Andres, C., Pertuy, D., Laroche, C., Pourcelot, Y., 2002. Dry powder inhaler: influence of humidity on topology and adhesion studied by AFM. Int. J. Pharm. 232 (1–2), 213–224.
Binnig, G., Quate, C.F., Gerber, Ch., 1986. Atomic force microscope. Phys. Rev. Lett. 56 (9), 930–933.
Buckton, G., 1997. Characterisation of small changes in the physical properties of powders of significance for dry powder inhaler formulations. Adv. Drug Deliv. Rev. 26 (1), 17–27.
Byrn, S.R., Lin, C.T., 1976. The effect of crystal packing and defects on desolvation of hydrate crystals of caffeine and L-(−)-1,4-cyclohexadiene-1-alanine. J. Am. Chem. Soc. 98 (13), 4004–4005.
Cui, Y., 2007. A material science perspective of pharmaceutical solids. Int. J. Pharm. 339 (1–2), 3–18.
Dalton, C.R., Hancock, B.C., 1997. Processing and storage effects on water vapor sorption by some model pharmaceutical solid dosage formulations. Int. J. Pharm. 156 (2), 143–151.
Edwards, H.G., Lawson, E., de Matas nd Len Shields, M., York, P., 1997. Metamorphosis of caffeine hydrate and anhydrous caffeine. J. Chem. Soc. Perkin Trans. 2 (10), 1985–1990.
Griesser, U.J., Burger, A., 1995. The effect of water vapor pressure on desolvation kinetics of caffeine 4/5-hydrate. Int. J. Pharm. 120 (1), 83–93.

Jones, M.D., Beezer, A.E., Buckton, G., 2008. Determination of outer layer and bulk dehydration kinetics of trehalose dihydrate using atomic force microscopy, gravimetric vapour sorption and near infrared spectroscopy. J. Pharm. Sci. 97 (10), 4404–4415.

Keel, T.R., Thompson, C., Davies, M.C., Tendler, S.J.B., Roberts, C.J., 2004. AFM studies of the crystallization and habit modification of an excipient material, adipic acid. Int. J. Pharm. 280 (1–2), 185–198.

Li, T., Morris, K., Park, K., 2000. Influence of solvent and crystalline supramolecular structure on the formation of etching patterns on acetaminophen single crystals: a study with atomic force microscopy and computer simulation. J. Phys. Chem. B 104 (9), 2019–2032.

Liu, X., Xu, D., Yu, G., Wang, X., Zhu, L., Zhang, G., Yu, G., 2007. Atomic force microscopy study on surface morphology of 0 0 1 faces of $[MnHg(SCN)_4(H_2O)_2].2C_4H_9NO$ crystals. Appl. Surf. Sci. 253 (7), 3674–3677.

Pirttimaki, J., Laine, E., 1994. The transformation of anhydrate and hydrate forms of caffeine at 100% RH and 0% RH. Eur. J. Pharm. Sci. 1 (4), 203–208.

Price, R., Young, P.M., 2004. Visualization of the crystallization of lactose from the amorphous state. J. Pharm. Sci. 93 (1), 155–164.

Roberts, C.J., 2005. What can we learn from atomic force microscopy adhesion measurements with single drug particles? Eur. J. Pharm. Sci. 24 (2–3), 153–157.

Thompson, C., Davies, M.C., Roberts, C.J., Tendler, S.J.B., Wilkinson, M.J., 2004. The effects of additives on the growth and morphology of paracetamol (acetaminophen) crystals. Int. J. Pharm. 280 (1–2), 137–150.

Tian, F., Sandler, N., Gordon, K., McGoverin, C.A., Reay, C.S., Saville, D., Rades, T., 2006. Visualizing the conversion of carbamazepine in aqueous suspension with and without the presence of excipients: a single crystal study using SEM and Raman microscopy. Eur. J. Pharm. Biopharm. 64 (3), 326–335.

Trask, A., Motherwell, W., Jones, W., 2005. Pharmaceutical cocrystallization: engineering a remedy for caffeine hydration. Cryst. Growth Des. 5 (3), 1013–1021.

Trask, A., 2007. An overview of pharmaceutical cocrystals as intellectual property. Mol. Pharm. 4 (3), 301–309.

Turner, Y.T.A., Roberts, C.J., Davies, M.C., 2007. Scanning probe microscopy in the field of drug delivery. Adv. Drug Deliv. Rev. 59 (14), 1453–1473.

Vishweshwar, P., McMahon, J.A., Bis, J.A., Zaworotko, M.J., 2006. Pharmaceutical cocrystals. J. Pharm. Sci. 95 (3), 499–516.